Cytoskeletal Organization of the Presynaptic Nerve Terminal and the Acetylcholine Receptor Cluster in Cell Cultures

H. BENJAMIN PENG
Department of Anatomy, University of Illinois College of Medicine, Chicago, Illinois 60680

ABSTRACT Whole-mount stereo electron microscopy has been used to examine the cytoskeletal organization of the presynaptic nerve terminal and the acetylcholine receptor (AChR) clusters in cultures of *Xenopus* nerve and muscle cells. The cells were grown on Formvar-coated gold electron microscope (EM) finder grids. AChR clusters were identified in live cultures by fluorescence microscopy after labeling with tetramethylrhodamine-conjugated α-bungarotoxin. After chemical fixation and critical-point drying, the cytoplasmic specializations of identified cells were examined in whole mount under an electron microscope. In the presynaptic nerve terminal opposite to the AChR cluster, synaptic vesicles were clearly suspended in a lattice of 5–12-nm filaments. Stereo microscopy showed that these filaments directly contacted the vesicles. This lattice was also contiguous with the filament bundle that formed the core of the axon. At the AChR cluster, an increased cytoplasmic density differentiated this area from the rest of the cytoplasm. This density was composed of a meshwork of filaments with a mean diameter of 6 nm and irregularly shaped membrane cisternae 0.1–0.5 μm in width, which resembled the smooth endoplasmic reticulum. These membrane structures were interconnected via the filaments. Organelles that were characteristic of the bulk of the sarcoplasm such as the rough endoplasmic reticulum and the polysomes, were absent from the cytoplasm associated with the AChR cluster. These results indicate that the cytoskeleton may play an important role in the development and/or the maintenance of the neuromuscular synapse, including the release of transmitter in the nerve terminal and the clustering of AChRs in the postsynaptic membrane.

One of the striking features of the structural specializations at the chemical synapse is an exact registration of the transmitter release mechanism at the presynaptic nerve terminal and the concentration of receptor molecules at the postsynaptic membrane (18). In the formation of neuromuscular junctions, such a registration is established very early (4). During subsequent stages of synaptogenesis, the relationship between the initially established pre- and postsynaptic elements appears to be stable (8). Thus there must be a mechanism to ensure the stabilization of these structures once they are formed.

The stability of the postsynaptic specialization, viz. the acetylcholine receptor (AChR)[1] clusters, has been demonstrated in cultured muscle cells. Diffusely distributed AChRs move freely in the plane of the plasma membrane (1, 27). However, when they are aggregated into clusters, this lateral mobility becomes severely restricted (1). The cluster often remains at the same location on the cell for extended period of time (20). This stability is maintained even when the cell is extracted with nonionic detergent Triton X-100 (28). This indicates that the cytoskeleton may be involved in the stabilization of AChR clusters. Morphologically, components of the cytoskeleton, in the form of cytoplasmic filaments, have been observed in close association with the AChR clusters in electron microscopic studies using thin-sectioning or freeze-etching techniques (5, 6, 12, 14, 26). In thin-section studies, one is limited to a two-dimensional image due to the small section thickness. Thus it is difficult to appreciate the relationship between the structural specializations associated with the AChR cluster and the overall cytoskeleton of the cell. In freeze-etching studies, the cells often need to be extracted so that the cytoplasm becomes etchable. Thus one is confronted with an inevitable loss of cytoplasmic organelles due to the extraction procedure.

The involvement of cytoskeleton in the organization of the

[1] *Abbreviations used in this paper:* AChR, acetylcholine receptor; EM, electron microscope; R-BTX, tetramethylrhodamine-conjugated α-bungarotoxin.

THE JOURNAL OF CELL BIOLOGY · VOLUME 97 AUGUST 1983 489-498

presynaptic nerve terminal has also been indicated in recent studies. In adrenal medulla Kondo et al. (17), using polyethylene glycol (PEG)-embedding method, has shown that the chromaffin granules appear to be suspended in a lattice composed of 3–12-nm filaments. Previous works on neuromuscular junctions (NMJs) have also suggested the existence of such a lattice in the cholinergic nerve terminal (11, 14). However, because of the tight packing of synaptic vesicles at adult NMJs, the filamentous connections between synaptic vesicles have not been resolved.

Tissue culture of neurons and muscle cells has greatly contributed to our understanding of synaptogenesis. Our previous studies on cultured *Xenopus* myotomal muscle cells have indicated that these cells are sufficiently thin such that their cytoskeletal organization could be resolved with whole-mount electron microscopy (25). In this study, we used this method to examine the three-dimensional cyto-architecture associated with the nerve terminal and the AChR clusters in cell cultures.

MATERIALS AND METHODS

Cell Cultures: Myotomal muscle cells were isolated from stage 20–22 *Xenopus laevis* embryos according to previous methods (15, 23). They were cultured on gold EM grids as detailed below in Steinberg's solution, consisting of 60 mM NaCl, 0.7 mM KCl, 0.4 mM $Ca(NO_3)_2$, 0.8 mM $MgSO_4$, and 10 mM *N*-2-hydroxyethylpiperazine-*N'*-2-ethanesulfonic acid (HEPES), pH 7.4, supplemented with 10% L-15 (Leibovitz) medium and 1% fetal bovine serum (Gibco Laboratories, Grand Island, NY). For nerve-muscle co-cultures, the myotomal cells were cultured together with isolated neural tube cells. The cultures were maintained at 22°C.

The gold grids used as culture substrate were prepared according to the method of Wolosewick and Porter (35). Briefly, 100-mesh gold EM finder grids (Ernest F. Fullam, Inc., Schenectady, NY) were coated with Formvar and picked up on no. 1 coverglass squares (18 mm × 18 mm), one grid per coverglass. The coverglass bearing the grid was then lightly shadowed with carbon and sterilized under UV.

Mapping the AChR Clusters: To locate the AChR clusters, the culture on the grid was labeled with tetramethylrhodamine-conjugated α-bungarotoxin (R-BTX) prepared according to Ravdin and Axelrod (29). Then it was mounted on a microscopic slide as shown in Fig. 1. The edges were sealed with dental wax. Fluorescence observation was carried out with a Leitz Orthoplan microscope equipped for epi-fluorescence, using a 40× or a 63× oil immersion objectives (N.A.1.3). The AChR clusters, as evidenced by intense R-BTX fluorescence, was recorded on Kodak Tri-X film, together with the phase-contrast image of the cell. The position of the cell with respect to the grid markings was used to identify the same cell under EM.

Whole-mount Electron Microscopy: After the sites of AChR clusters were identified, the culture was removed from the slide and fixed with 0.5% glutaraldehyde in 0.05 M Na-cacodylate buffer (pH 7.2) overnight at 4°C and postfixed with 1% OsO_4 for 10 min at 22°C. Then the grid was removed from the coverglass and placed in a specially constructed grid holder (35). It was dehydrated through an ethanol series and critical point-dried through CO_2. A thin layer of carbon was then deposited on both sides of the grid to provide stability during observation. Cells previously identified with light microscopy were examined with a JEOL 100 CX electron microscope equipped with a side-entry goniometer stage at 100 kV or with an AEI high-voltage electron microscope at 1,000 kV (located at Madison, WI). The stereo micrographs presented in this paper can be viewed with a stereoscopic binocular lens.

The acceleration voltage was 100 kV for all the figures except Fig. 9, which was taken at 1,000 kV.

RESULTS

During the course of this work, 300 muscle cells in more than 10 different cultures were examined by fluorescence microscopy followed by whole-mount EM. 20 cells were sufficiently thin for EM imaging. These cells were carefully photographed and the whole-mount images of the AChR cluster sites were compared with their fluorescence images. The criteria for the sample selection are as follows. On the AChR clusters, the area of the cytoplasmic specialization as seen in the whole-mount EM image at low magnification (see Fig. 8*c*) has to match the area of R-BTX fluorescence image (see Fig. 8*b*) both in size and in shape. On the presynaptic specialization, the nerve terminal has to be immediately adjacent to a postsynaptic AChR cluster as shown by R-BTX fluorescence (Figs. 2*b* and 5*b*) and synaptic vesicles, which are defined as spherical, membrane-bound structures ~50–60 nm in diameter based on previous thin-sectioning data (24), must be clearly present in the terminal (see Figs. 3 and 6) in whole-mount images. Since cell thickness tends to increase with the culture age, the observation was restricted to cultures 1–2 d old. The details of three cells are presented in this report, two on the presynaptic nerve terminal and one on the AChR cluster. However, the same types of specializations were seen in all other preparations selected according to above criteria.

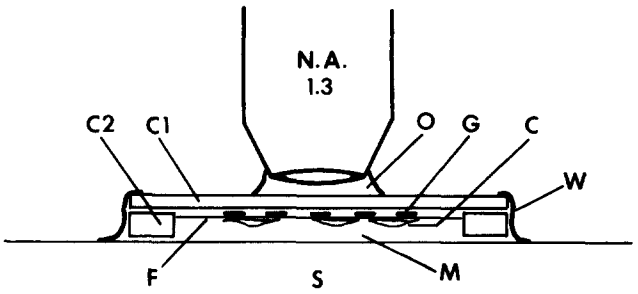

FIGURE 1 Assembly of the cell culture for mapping the AChR clusters. The cells (*C*) were grown on gold EM finder grid (*G*), coated with Formvar (*F*) and carbon. The grid was carried by a no. 1 coverglass (*C1*). After R-BTX labeling, the live culture was inverted on a slide (*S*) and was supported by two strips of no. 2 coverglass (*C2*). The four edges were sealed with dental wax (*W*) such that a small amount of culture medium (*M*) was enclosed. Epifluorescence observation was made through an oil (*O*)-immersion 40X or 63X objective with N.A. 1.3.

Presynaptic Nerve Terminal

Two kinds of nerve-muscle contacts were observed: the synapse was either located at a terminal bouton (Fig. 2) or along the length of the axon (see Fig. 5).

Fig. 2*a* shows the phase-contrast image of a nerve-muscle contact and Fig. 2*b* shows the location of the AChR clusters as indicated by R-BTX fluorescence. By comparing the landmarks, including the grid bars and objects displaying a broad spectrum of auto-fluorescence such as the yolk granules, one could locate the sites of AChR clusters as shown in Fig. 2*b* exactly on the phase-contrast image. Two prominent clusters and a third faintly fluorescent cluster were located along the periphery of the muscle cell (Fig. 2*b*). The whole-mount EM image was shown in Fig. 2*c*. By comparing with the phase-contrast image (Fig. 2*a*), the location of the synapse as shown by R-BTX staining can be readily located on the EM image (Fig. 2*c*). What appears to be a single neurite in Fig. 2*a* was actually composed of a series of neuritic extensions. Terminal 1 was directly opposite to an AChR cluster and made a close contact with the muscle cell. In contrast, terminal 2, despite its proximity to an AChR cluster, was not in direct contact with the muscle cell. Detailed images of terminal 1 are presented below.

Fig. 3 shows terminal 1 in stereo. This terminal measured 2.3 μm long and 1.4 μm wide. Toward the top of Fig. 3, it was continuous with an axon. Toward the bottom of Fig. 3,

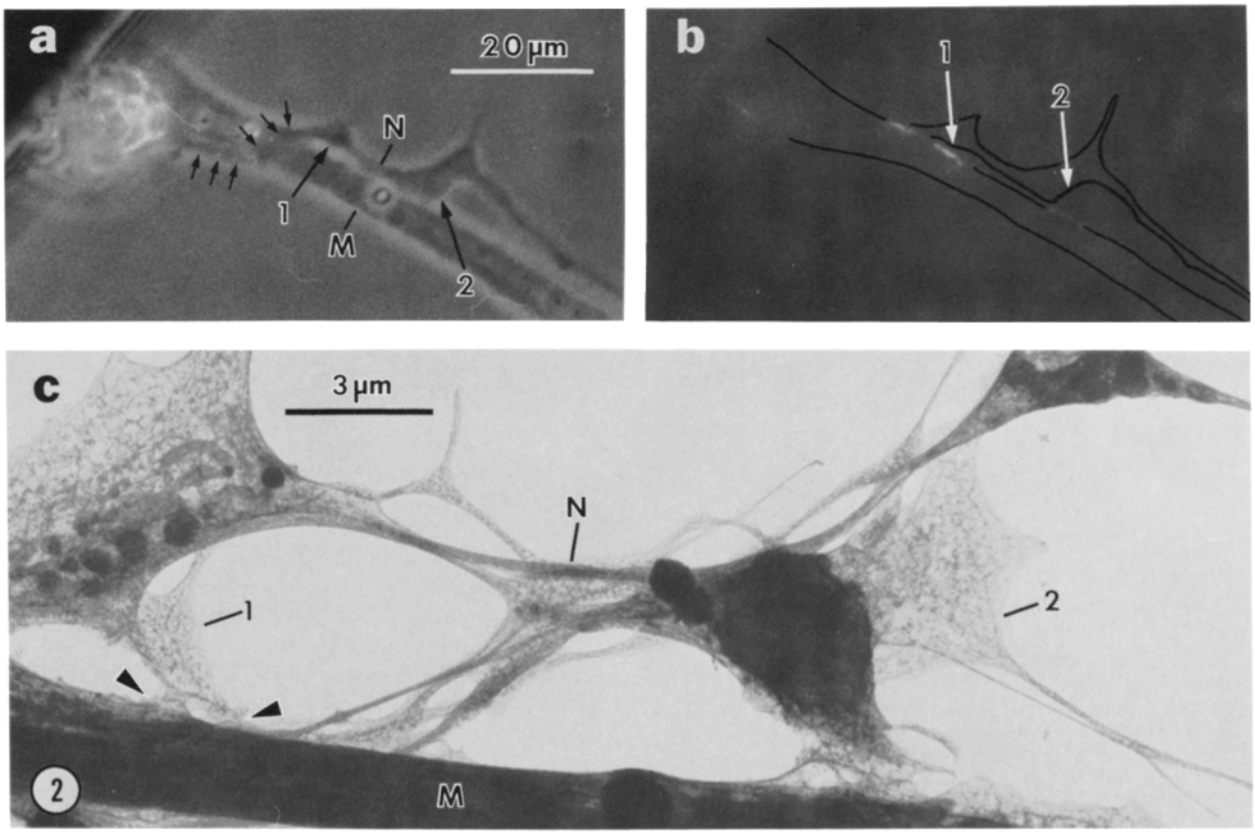

FIGURE 2 A nerve-muscle contact which was associated with AChR clusters. (*a*) Phase contrast; (*b*) fluorescence; (*c*) whole-mount EM. The cells were outlined in *b*. Small arrows in *a* point to the neuritic path. The nerve crossed the muscle at the left of *a* and, as it emerged from the other side, became associated with three AChR clusters as shown by R-BTX fluorescence (*b*). The positions of terminals 1 and 2 in *c* are pointed out in *a* and *b*. Terminal 1 was in direct contact with the muscle cell whereas terminal 2 was not. Arrowheads in *c* point to the sites of closest nerve-muscle contact. *N*, nerve; *M*, muscle. (*a* and *b*) × 960. (*c*) × 6,500.

this terminal made contact with the muscle.

The most prominent feature of this nerve terminal was the presence of numerous synaptic vesicles (arrowheads in Fig. 3), which had a mean diameter of 54 nm (SD = 13 nm, n = 21). They appeared to be evenly distributed throughout the terminal, without particular clustering at the nerve-muscle contact. These vesicles were clearly suspended in a lattice composed of cytoplasmic filaments (Fig. 3). In stereo (Fig. 4), one can see that these filaments made direct contact with the vesicles. The diameter of the filaments ranged from 5–12 nm (mean = 9 nm, SD = 2.5 nm, n = 17) and each filament segment was 0.1 to 0.2 μm in length. They interconnected the vesicles and also made attachments to the cell margin (Fig. 3).

A different type of synapse, by which the nerve contacted the muscle cell along its length, is shown in Fig. 5. The nerve made contact with the muscle cell at two places (Fig. 5*a*) and each was associated with an AChR cluster (Fig. 5*b*). The corresponding EM image is seen in Fig. 5*c*. The second synaptic position was located at a thick portion of the muscle cell and therefore was not further imaged. Fig. 6 shows the first contact at a higher magnification. This neurite made a varicosity at the nerve-muscle contact and the presynaptic membrane partially overlapped the muscle at this synapse. The AChR cluster measured 8 μm in length, which was approximately equal to the length of the neurite where synaptic vesicles were seen (Figs. 5*c* and 6). The core of the axon was occupied by a bundle of longitudinally oriented filaments which measured 11–14 nm in diameter (Figs. 6 and 7). Away from the presynaptic membrane, the varicosity was much simpler in organization and appeared quite transparent (Fig. 6).

The synaptic vesicles with a mean diameter of 65 nm (SD = 10 nm, n = 22) were concentrated at the site where the nerve made a close contact with the muscle (Figs. 6 and 7), immediately adjacent to an AChR cluster. These vesicles were suspended in a lattice composed of 5–12-nm filaments (Fig. 7). Direct contacts between these filaments and the vesicles were clearly observed (Fig. 7). This filamentous lattice was seen throughout the area where synaptic vesicles were located.

ACh Receptor Clusters

In most of the nerve-muscle contacts we have examined, there was an overlap between the pre- and postsynaptic membranes (e.g., Fig. 6). This overlap obscured the fine structures of the postsynaptic specializations. Thus we chose to examine the ultrastructure of the AChR clusters not in contact with the nerve, the "hot spots."

Fig. 8*a* and *b* show an AChR cluster located along the edge of a muscle cell opposite to a melanocyte as evidenced by R-BTX labeling. Its whole-mount EM image is shown in Fig. 8*c*, which is at eight times the magnification of Fig. 8*a* and *b*. Even at this relatively low magnification, an area of increased cytoplasmic density that corresponds both in size and in shape with the AChR cluster (Fig. 8*b*) can be observed. Thus, in such areas where the thickness of the cell was minimal, the location of the AChR cluster could be unambiguously identified in these electron micrographs.

Fig. 9 shows a portion of the sub-AChR cluster cytoplasm in stereo. It is apparent that this cytoplasmic area was occupied by two components: a meshwork of filaments and a set of membrane-bound cisternae. These cisternae, having a width of 0.1 to 0.5 μm, resembled smooth endoplasmic reticulum (SER). In fact, they often extended beyond the area occupied by the AChR cluster as defined by the fluorescent R-BTX image. They were interconnected to each other either through a membranous extension or via a filamentous linkage as shown in this high voltage electron micrograph (Fig. 9). Fig. 10 is a conventional 100 kV micrograph that shows the filaments and the cisternae in a better contrast. One can see

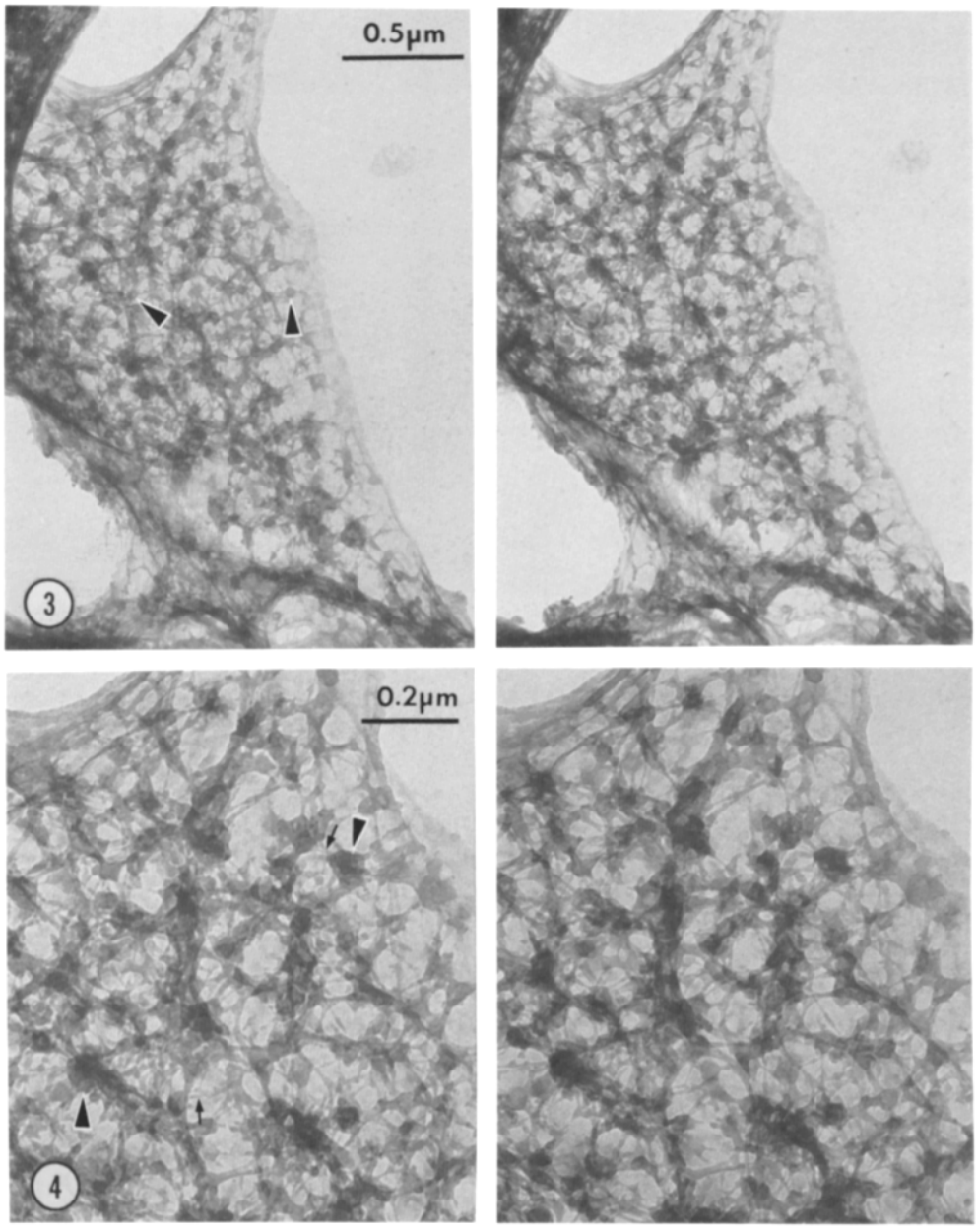

FIGURES 3 and 4 Fig. 3: Stereo view of the entire terminal 1 as shown in Fig. 2c. This terminal synapsed with the muscle at the bottom and was continuous with its axon toward the top. Arrowheads point to synaptic vesicles. Tilt angle = 30°. Fig. 4: Stereo view of a portion of terminal 1 in Fig. 2c. Synaptic vesicles (arrowheads) are suspended in a filamentous lattaice. These filaments often made direct contacts with the vesicles as indicated by small arrows. Tilt angle = 15°. Fig. 3, × 32,500; Fig. 4, × 65,000.

FIGURES 5 and 6 Fig. 5: A synapse formed along the length of the axon. (*a*) Phase contrast; (*b*) fluorescence; (*c*) whole-mount EM. Two AChR clusters were formed along the nerve-muscle contacts (*b*). The top contact is imaged in *c*. Two yolk granules (asterisks in *a* and *c*) were used as landmarks to locate precisely the position of this AChR cluster. *N*, nerve; *M*, muscle. Fig. 6: Stereo view of the nerve-muscle contact shown in Fig. 5*c*. The axon made a varicosity at this site. Within the varicosity, the cytoplasm was rather transparent. The core of the axon (*A*) was occupied by a bundle of 11–14-nm filaments. Opposite to the varicosity was the presynaptic area which contained many synaptic vesicles. This area is directly opposite to an AChR cluster as shown in Fig. 5. Arrowheads point to the boundary of the neurite. The presynaptic area partly overlapped the postsynaptic area. *mi*, mitochondrion. Tilt angle = 20°. Fig. 5: (*a–b*) × 960; (*c*) × 6,500. Fig. 6 × 14,500.

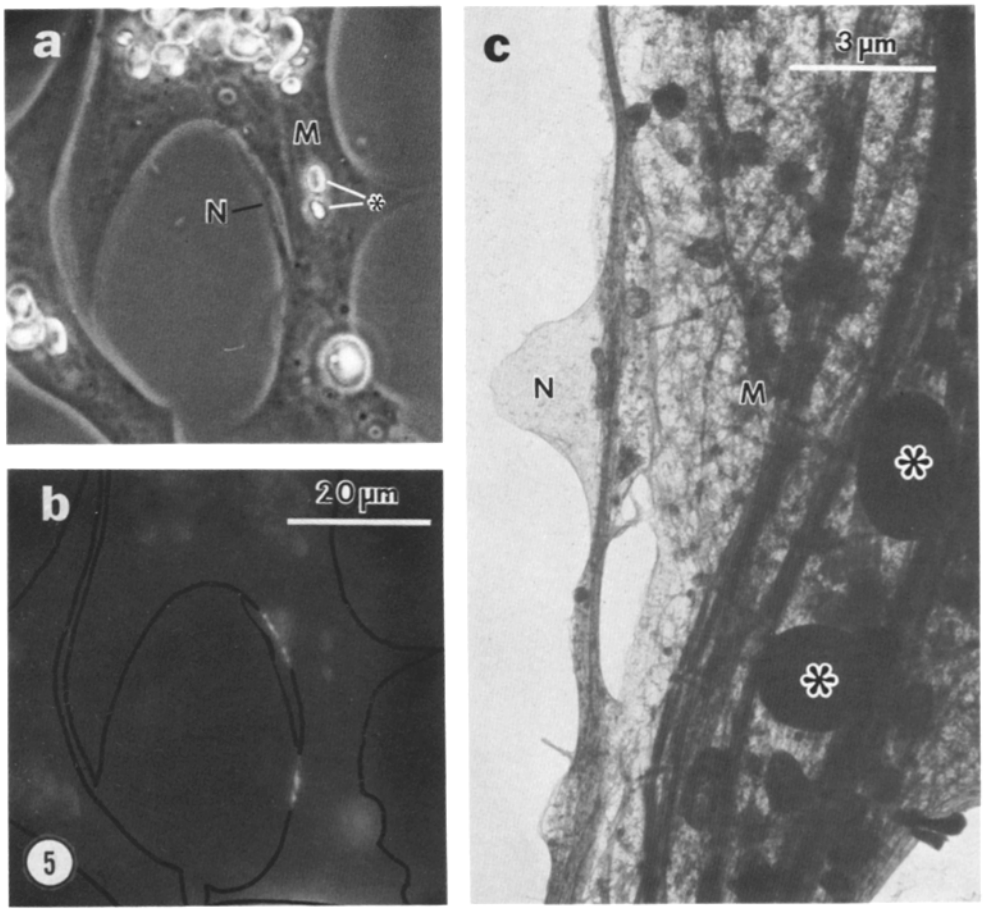
a
M
N
b
20 μm
5
c
3 μm
N
M

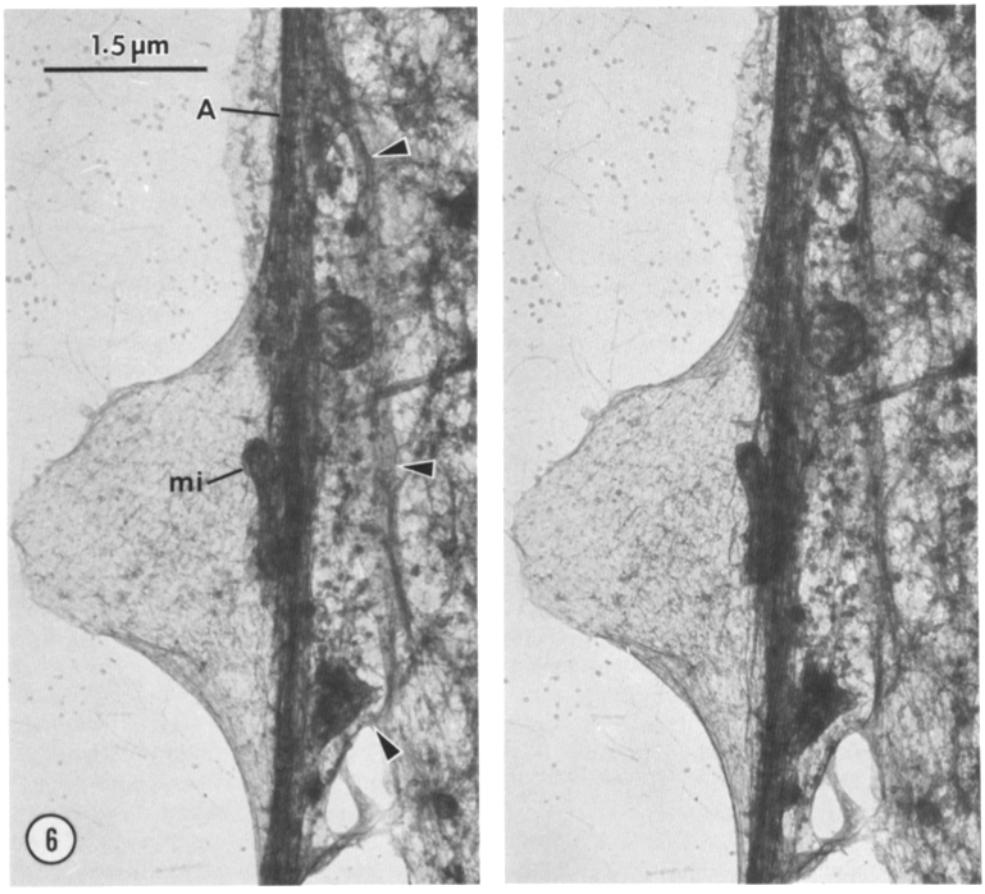
1.5 μm
A
mi
6

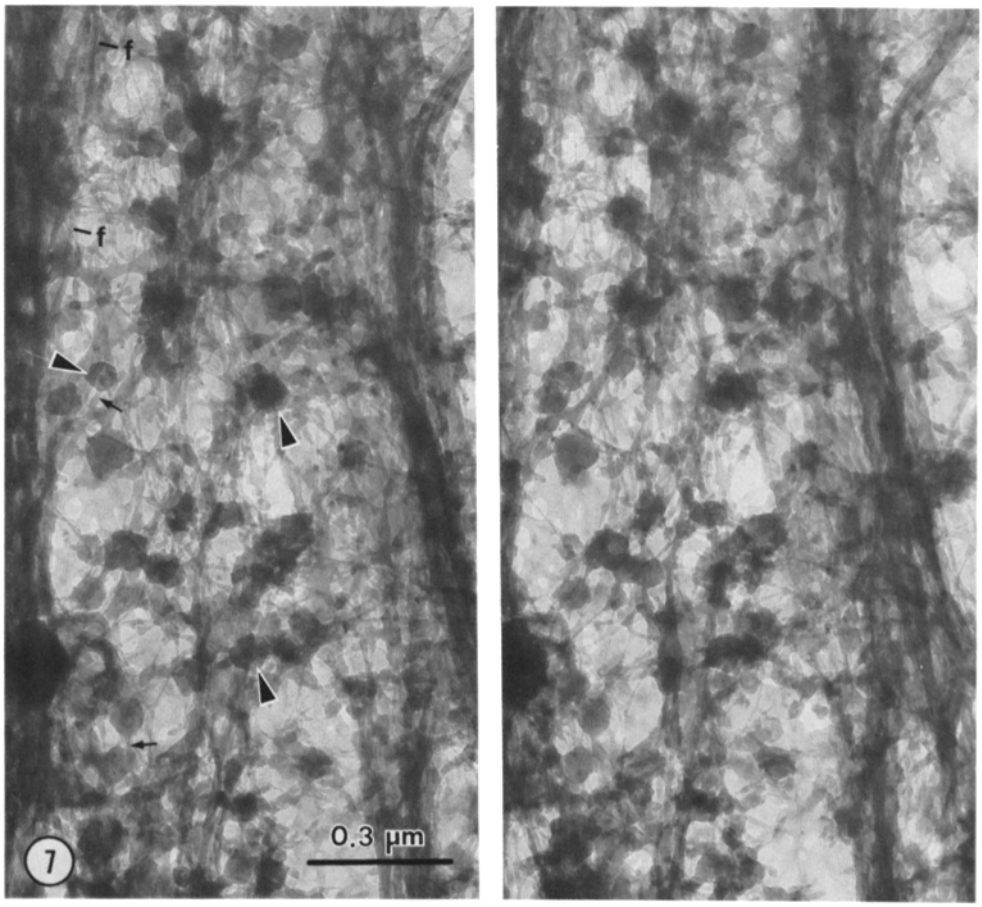

FIGURE 7 Presynaptic specializations of Fig. 6 at a higher magnification, stereo view. Synaptic vesicles (arrowheads) were suspended in a filamentous lattice which pervaded the entire presynaptic axoplasm. Direct contacts between the vesicles and the filaments are indicated by small arrows. Longitudinally running 11–14-nm filaments (*f*) also contributed to this lattice. Tilt angle = 15°. × 65,000.

that the filaments often converged onto the cisternae. Although the rough endoplasmic reticulum (RER) and polysomes were commonly observed in the cytoplasm away from the AChR clusters (Fig. 11), they were absent from the cytoplasm at the cluster (Fig. 9).

The filaments forming the meshwork at the AChR cluster ranged from 3 nm to 10 nm in diameter with a mean of 6 nm (SD = 2.7 nm, n = 10). The complex meshwork formed by these filaments, together with the membrane cisternae, contributed to the increased cytoplasmic density observed at the AChR cluster in whole-mount (Fig. 8*c*).

Coated vesicles or pits with a diameter of 0.1 μm were also observed in the area occupied by the AChR cluster (Fig. 9). The "coat" was often associated with the filament meshwork described above (Fig. 9).

As a control, we have examined areas of the same cell not in association with the AChR cluster. One such area is shown in Fig. 11. The cytoplasmic organization was much less complicated than at the AChR cluster. SER, RER, and polysomes were present. Bundles of 6-8-nm filaments were observed both in the cytoplasm as well as in association with the cell cortex and intermediate (10 nm) filaments were also present. The cytoplasm between the organelles was occupied by a lattice composed of 3–4-nm filaments, which appears to be similar to the microtrabecular lattice observed in nonmuscle cells (34).

DISCUSSION

In this study we have demonstrated that a three-dimensional cytoskeletal lattice exists both in the presynaptic nerve terminal and at the AChR cluster in developing nerve-muscle cocultures. Although we were unable to obtain images of the postsynaptic specializations due to the overlapping of the pre- and postsynaptic structures, the AChR cluster should provide a close analogy. Structures typically associated with the postsynaptic area at the neuromuscular junction, e.g., the membrane-associated cytoplasmic density, the basal lamina, and the concentration of cholinesterase, are also observed at the AChR clusters (3, 26, 33).

Whole-mount EM of chemically fixed, critical point-dried specimens were examined in this study. Since the cells were not extracted with detergent, presumably a larger portion of the cytoskeleton was left intact than the extracted preparations. Fluorescence microscopy with R-BTX enabled us to identify the sites of synaptic structures yet without obscuring their fine details under electron microscopy. In this respect, our attempt to demonstrate these synaptic specializations by whole-mount EM in conjunction with horseradish peroxidase (HRP)-conjugated α-bungarotoxin (19) was not successful, mainly due to the lack of a high specificity of this label to the AChRs and the fact that the electron density of the reaction product often obscured the underlying structures.

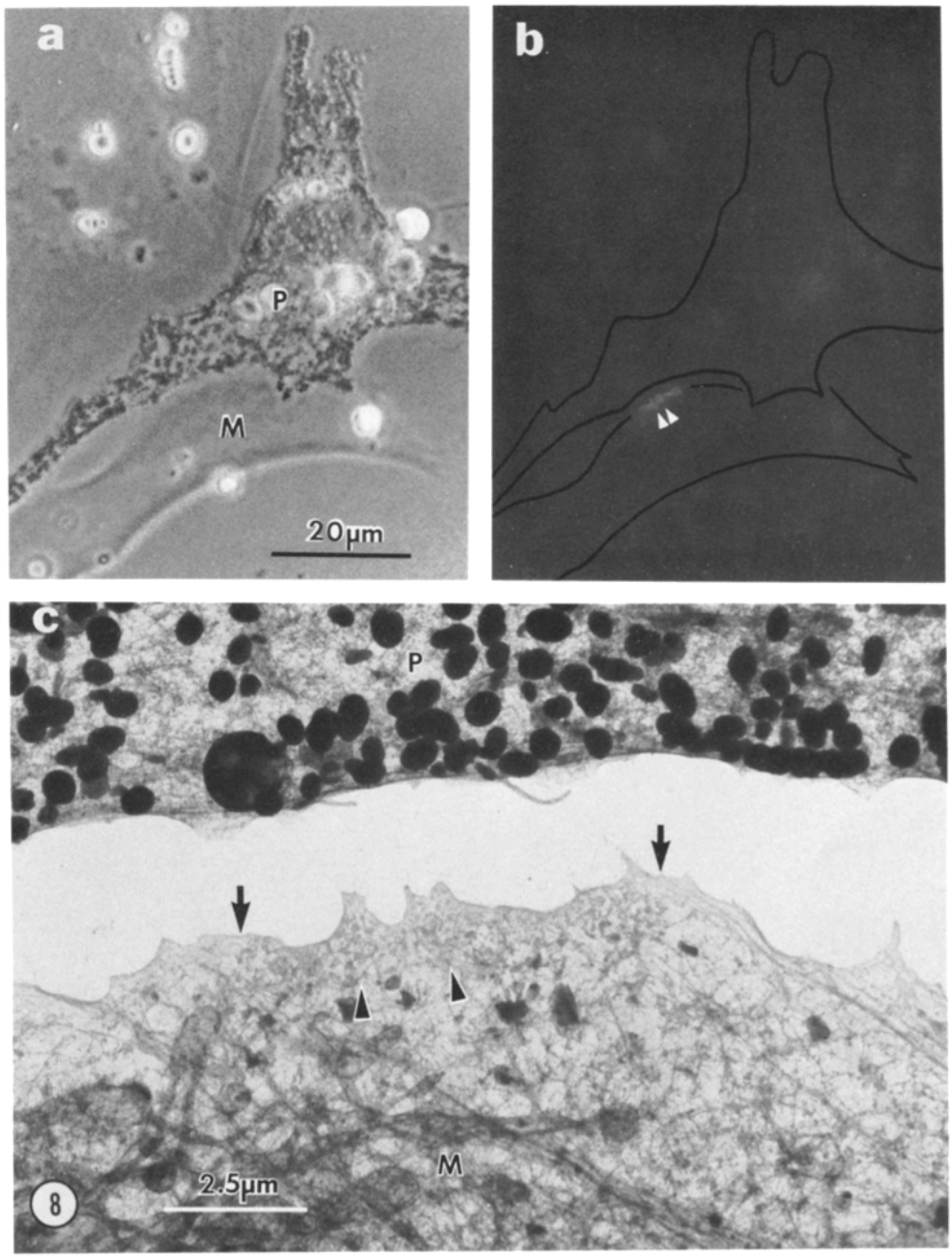

FIGURE 8 An AChR cluster located at the cell margin. *a*, phase-contrast; *b*, fluorescence; *c*, whole-mount EM. The muscle cell (*M*) is opposite to a melanocyte (*P*). The R-BTX image of the AChR cluster in *b* matches well with the area of increased cytoplasmic density in *c* (between arrows), both in size and in shape. The two cytoplasmic projections as pointed out by arrowheads in *b* are reproduced in *c* (arrowheads). This area of cytoplasmic specialization at the AChR cluster is in sharp contrast to the surrounding area where diffuse AChRs reside. (*a* and *b*) × 960; (*c*) × 7,800.

Presynaptic Specializations

In this study, we relied on the fluorescence of R-BTX staining to indicate the functionality of the nerve-muscle synapse (Figs. 2 and 5). Although the physiology of synaptic transmission was not tested, it is known that functional synapses develop quickly in these *Xenopus* nerve-muscle cocultures (24) and Kidokoro et al. (16) have shown that AChR clustering is *always* associated with miniature endplate potentials. Thus, the neuromuscular contacts which were AChR cluster-positive (Figs. 2 and 5) should have been physiologically functional, despite a lack of clustering of synaptic vesicles at the presynaptic membrane (Fig. 3). Other studies (21, 24) using thin-sectioning and physiological methods, have also shown that the onset of neuromuscular transmission precedes the presynaptic clustering of vesicles.

In the axon, a system of cross connections among membranous organelles, microtubules, and neurofilaments has been documented (7, 13, 30). This work has shown that such a cross-linker system also extends to the presynaptic nerve terminal (Fig. 3 and 4). Within the terminals, this system cross-links the synaptic vesicles. The function of such connections is unknown. However, this system should now be taken into consideration in our understanding of the translocation of synaptic vesicles during transmission at neuromuscular junctions.

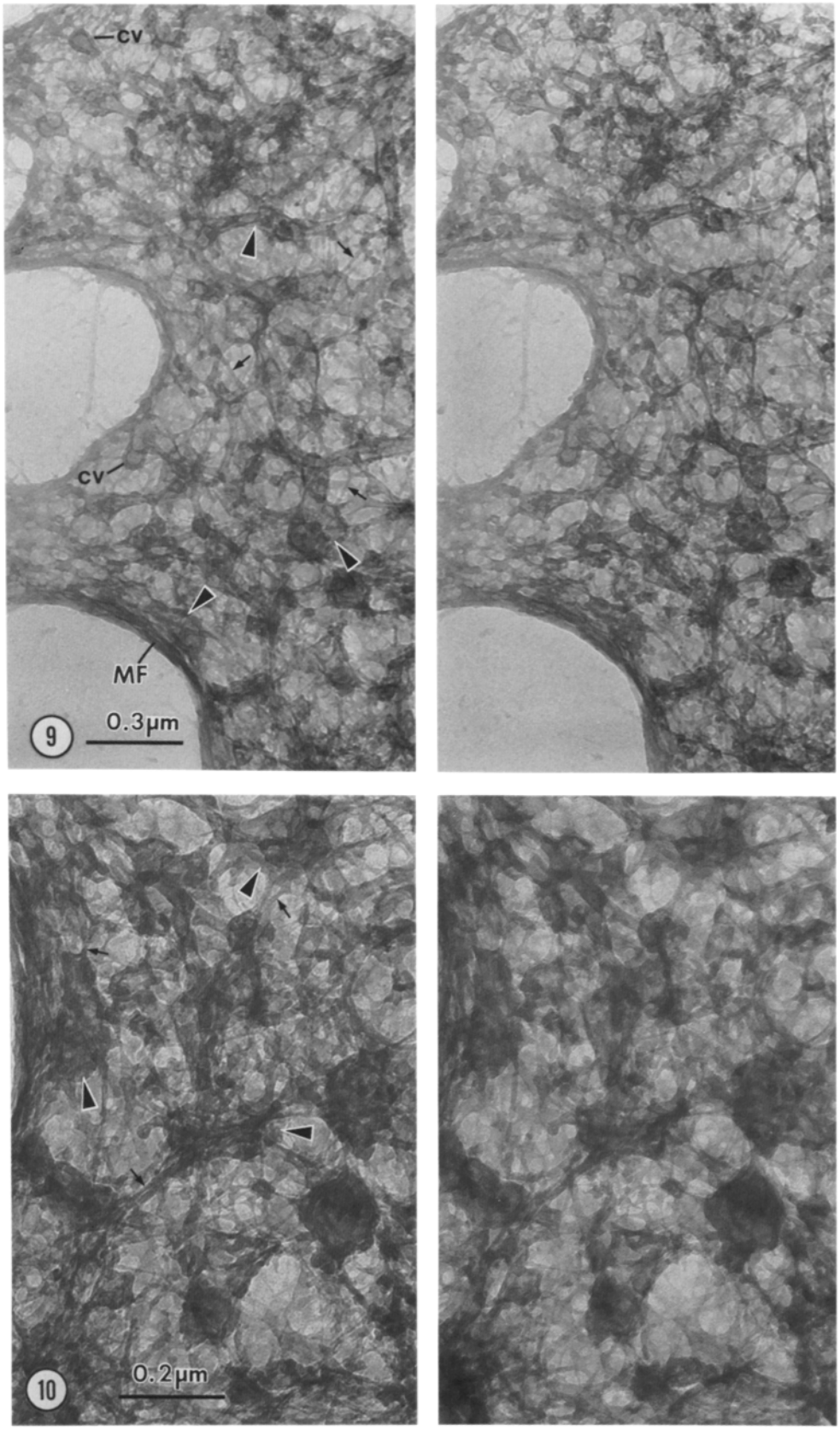

FIGURES 9 and 10 Fig. 9: Stereo view of a portion of the AChR cluster shown in Fig. 8. Membrane cisternae (arrowheads) and a meshwork of filaments (arrows) together contributed to the cytoplasmic specialization. A bundle of thin filaments (*MF*) was located along the margin of the cell. Two coated vesicles or pits (*CV*) can be seen in this field. Tilt angle = 10°; acceleration voltage = 1,000 kV. Fig. 10. An enlarged view (rotated 90°) of Fig. 9. This 100 kV image offers a better contrast of the filament meshwork than Fig. 9. The filaments (arrows) and the membrane cisternae (arrowheads) were often interconnected. Tilt angle = 10°. Fig. 9, × 50,000. Fig. 10, × 82,500.

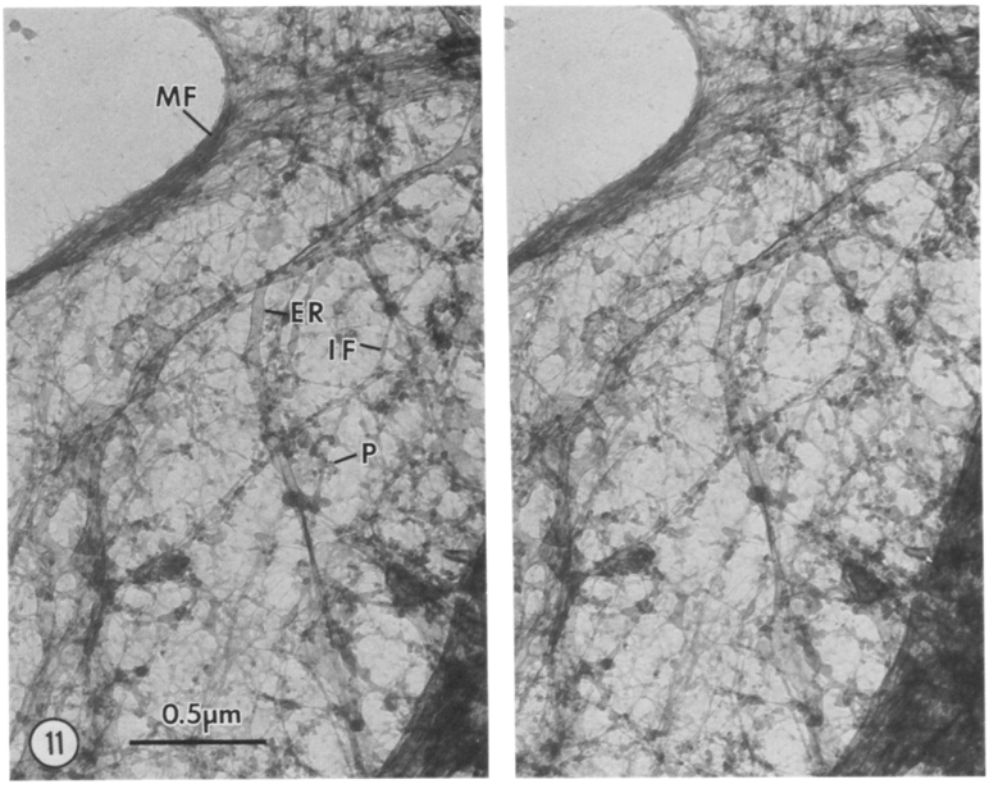

FIGURE 11 An area of the cytoplasm away from the AChR cluster from the same muscle cell shown in Figs. 8–10, stereo view. The cytoplasm appeared less dense than at the AChR cluster. Bundles of microfilaments (*MF*), 10-nm filaments (*IF*), endoplasmic reticulum (*ER*), and polysomes (*P*) were prominent structures in the cytoplasm. Tilt angle = 10°. × 36,000.

AChR Clusters

We have also shown that a three-dimensional meshwork of filaments is associated with the AChR cluster. Although this meshwork is contiguous with the cytoskeleton of the cell, it is unique to the area of the receptor cluster. In the cluster-free area the organization of the cytoskeleton is much simpler (Fig. 11). Our work, however, has not shown how individual receptors within the cluster are linked to the filament meshwork. In freeze-etching studies on the postsynaptic membrane of anteroventral cochlear nucleus (AVCN), Gulley and Reese (9) provided evidence that the putative receptor intramembranous particles are associated with 4-nm filaments on the cytoplasmic side. In thin-section studies on AChR clusters in cultured *Xenopus* muscle cells, Peng and Cheng (see Fig. 9, *inset*, in reference 26) have also observed that putative AChR particles are associated with 3–5-nm cytoplasmic filaments. Perhaps these filaments provide the link between the membrane-embedded receptors and the meshwork of filaments reported here.

A submembranous meshwork of filaments has also been demonstrated by a variety of other techniques in a number of different postsynaptic membranes, including adult neuromuscular junctions (6, 14), *Torpedo* (12), and AVCN (9). Current evidence indicates that it is the prime candidate for the machinery that restricts the lateral mobility of clustered receptors within the plane of the membrane. Diffuse AChRs, which reside in the cluster-free area of the membrane in cultured muscle cells, have a high lateral diffusion coefficient (1, 27) and correspondingly are not associated with such a filamentous meshwork (Fig. 11).

Our work has also revealed that, in addition to cytoplasmic filaments, a system of interconnected membranous cisternae (Figs. 9 and 10) is also an intergral component of the AChR cluster-associated specializations. These structures often form the loci for the attachment of filaments (Fig. 10). Previously, Ornberg and Reese (22) have provided evidence for the existence of such membrane cisternae in the subsynaptic cytoplasm of skeletal muscle. Their data suggested a Ca^{2+} sequestering role for these membrane-bound structures.

The identity of the filaments in the meshwork is unknown. The average sizes of these filaments in this work (6 nm) and in others works (5–10 nm in reference 12; 8–9 nm in reference 9) indicate that they could be actin filaments. Hall et al. (10), with immunofluorescence techniques using an antibody against cytoplasmic actin, have shown that actin is concentrated at the endplates. This further suggests that the meshwork may be composed of F actin. A meshwork of F actin also exists at the leading edge of migrating nonmuscle cells (2, 31, 32), where the cell engages in motility-oriented activities such as membrane ruffling. Thus, in addition to the stabilization of individual receptors, the filamentous meshwork associated with the AChR cluster may also be involved in receptor movements during synaptogenesis.

I wish to thank Dr. Douglas Fambrough for providing fluorescently conjugated α-bungarotoxin at the early phase of this study.

This work was supported by National Institutes of Health (NIH) grant NS16259 and a grant from the Muscular Dystrophy Association.

Received for publication 29 November 1982, and in revised form 28 April 1983.

REFERENCES

1. Axelrod, D., P. Ravdin, D. E. Koppel, J. Schlessinger, W. W. Webb, E. L. Elson, and T. R. Podleski. 1976. Lateral motion of fluorescently labeled acetylcholine receptors in membranes of developing muscle fibers. *Proc. Natl. Acad. Sci. USA.* 73:4954–4958.

2. Buckley, I. K., and K. R. Porter. 1967. Cytoplasmic fibrils in living cultured cells. *Protoplasma.* 64:349–380.
3. Burrage, T. G., and T. L. Lentz. 1981. Ultrastructural characterization of surface specializations containing high-density acetylcholine receptors on embryonic chick myotubes *in vivo* and *in vitro*. *Dev. Biol.* 85:267–286.
4. Cohen, S. A., and G. D. Fischbach. 1977. Clusters of acetylcholine receptors located at identified nerve-muscle synapses *in vitro*. *Dev. Biol.* 59:24–38.
5. Couteaux, R., and M. Pecot-Dechavassine. 1968. Particularities structurales due sarcoplasme sous-neural. *C. R. Acad. Sci. (Paris).* 266:D8–D10.
6. Ellisman, M. H., J. E. Rash, L. A. Staehelin, and K. R. Porter. 1976. Studies of excitable membranes. II. A comparison of specializations at neuromuscular junctions and nonjunctional sarcolemmas of mammalian fast and slow twitch muscle fibers. *J. Cell Biol.* 68:752:754.
7. Ellisman, M. H., and K. R. Porter. 1980. Microtrabecular structure of the axoplasmic matrix: visualization of cross-linking structures and their distribution. *J. Cell Biol.* 87:464–479.
8. Frank, E., and G. D. Fischbach. 1979. Early events in neuromuscular junction formation *in vitro*. *J. Cell Biol.* 83:143–158.
9. Gulley, R. L., and T. S. Reese. 1981. Cytoskeletal organization at the postsynaptic complex. *J. Cell Biol.* 91:298–302.
10. Hall, Z. W., B. W. Lubit, and J. H. Schwartz. 1981. Cytoplasmic actin in postsynaptic structures at the neuromuscular junction. *J. Cell Biol.* 90:789–792.
11. Heuser, J. 1980. 3-D visualization of membrane and cytoplasmic specializations at the frog neuromuscular junction. *In* Ontogenesis and Functional Mechanisms of Peripheral Synapses. J. Taxi, editor. Elsevier/North-Holland, Amsterdam. 139–155.
12. Heuser, J. E., and S. R. Salpeter. 1979. Organization of acetylcholine receptors in quick-frozen, deep-etched and rotary-replicated *Torpedo* postsynaptic membrane. *J. Cell Biol.* 82:150–173.
13. Hirokawa, N. 1982. Cross-linker system between neurofilaments, microtubules, and membranous organelles in frog axons revealed by the quick-freeze, deep-etching method. *J. Cell Biol.* 94:129–142.
14. Hirokawa, N., and J. E. Heuser. 1982. Internal and external differentiations of the postsynaptic membrane of the neuromuscular junction. *J. Neurocytol.* 11:487–510.
15. Jones, K. W., and T. R. Elsdale. 1963. The culture of small aggregates of amphibian embryonic cells *in vitro*. *J. Embryol. Exp. Morphol.* 11:135–154.
16. Kidokoro, Y., M. J. Anderson, and R. Gruener. 1980. Change in synaptic potential properties during acetylcholine receptor accumulation and neurospecific interactions in *Xenopus* nerve-muscle cell culture. *Dev. Biol.* 78:464–483.
17. Kondo, H., J. J. Wolosewick, and G. D. Pappas. 1982. The microtrabecular lattice of the adrenal medulla revealed by polyethylene glycol embedding and stereo electron microscopy. *J. Neurosci.* 2:57–65.
18. Kuffler, S. W., and J. G. Nicholls. 1976. From neuron to brain. Sinauer Associates. Sunderland, MA 192–218.
19. Lentz, T. L., J. E. Mazurkiewicz, and J. Rosenthal. 1977. Cytochemical localization of acetylcholine receptors at the neuromuscular junction by means of horseradish peroxidase-labeled α-bungarotoxin. *Brain Res.* 132:423–442.
20. Moody-Corbett, F., and M. W. Cohen. 1982. Influence of nerve on the formation and survival of acetylcholine receptor and cholinesterase patches on embryonic *Xenopus* muscle cells in culture. *J. Neurosci.* 2:633–646.
21. Nakajima, Y., T. Takahashi, K. Hirokawa, S. Nakajima, and K. Onedera. 1982. Ultrastructural and physiological properties of functional neuromuscular junctions in *Xenopus* cell culture. *J. Cell Biol.* 95:2*a*. (Abstr.).
22. Ornberg, R. L., and T. S. Reese. 1980. A freeze-substitution method for localizing divalent cations: examples from secretory systems. *Fed. Proc.* 39:2802–2808.
23. Peng, H. B., and Y. Nakajima. 1978. Membrane particle aggregates in innervated and noninnervated cultures of *Xenopus* embryonic muscle cells. *Proc. Natl. Acad. Sci. USA.* 75:500–504.
24. Peng, H. B., P. C. Bridgman, S. Nakajima, A. Greenberg, and Y. Nakajima. 1979. A fast development of presynaptic function and structure of the neuromuscular junction in *Xenopus* tissue culture. *Brain Res.* 167:379–384.
25. Peng, H. B., J. J. Wolosewick, and P.-C. Cheng. 1981. The development of myofibrils in cultured muscle cells: a whole-mount and thin-section electron microscopic study. *Dev. Biol.* 88:121–136.
26. Peng, H. B., and P.-C. Cheng. 1982. Formation of postsynaptic specializations induced by latex beads in cultured muscle cells. *J. Neurosci.* 2:1760–1774.
27. Poo, M.-M. 1982. Rapid lateral diffusion of functional ACh receptors in embryonic muscle cell membrane. *Nature (Lond.).* 295:332–334.
28. Prives, J., A. B. Fulton, S. Penman, M. P. Daniels, and C. N. Christian. 1982. Interaction of the cytoskeletal framework with acetylcholine receptor on the surface of embryonic muscle cells in culture. *J. Cell Biol.* 92:231–236.
29. Ravdin, P., and D. Axelrod. 1977. Fluorescent tetramethyl rhodamine derivatives of α-bungarotoxin: preparation, separation and characterization. *Anal. Biochem.* 80:585–592.
30. Schnapp, B. J., and T. S. Reese. 1982. Cytoplasmic structure in rapid-frozen axons. *J. Cell Biol.* 94:667–679.
31. Small, J. V. 1981. Organization of actin in the leading edge of cultured cells: influence of osmium tetroxide and dehydration on the ultrastructure of actin meshwork. *J. Cell Biol.* 91:695–705.
32. Small, J. V., G. Isenberg, and J. E. Celis. 1978. Polarity of actin at the leading edge of cultured cells. *Nature (Lond.).* 272:638–639.
33. Weldon, P. R., F. Moody-Corbett, and M. W. Cohen. 1981. Ultrastructure of sites of cholinesterase activity on amphibian embryonic muscle cells cultured without nerve. *Dev. Biol.* 84:341–350.
34. Wolosewick, J. J., and K. R. Porter. 1976. Stereo high-voltage electron microscopy of whole cells of the human diploid lines, WI-38. *Am. J. Anat.* 147:303–323.
35. Wolosewick, J. J., and K. R. Porter. 1979. Preparation of cultured cells for electron microscopy. *In* Practical Tissue Culture Applications. K. Maramorsch and H. Hirumi, editors. Academic Press, New York. 59–85.